



Utilizing Recovered Carbon Black as a Reinforcing Agent for Ethylene Propylene Diene Rubber Formulation

Onur Yucak ^{1*}, Deniz Uzunsoy ¹, Halit Levent Hosgun ²

¹ Bursa Technical University, Department of Metallurgical and Materials Engineering, 16310, Bursa, Türkiye

² Bursa Technical University, Department of Chemical Engineering, 16310, Bursa, Türkiye

ARTICLE INFO

Received Date: 17/04/2025
Accepted Date: 4/07/2025

Cite this paper as:

Yucak O., Uzunsoy D. & Hosgun H. L. (2026). Utilizing Recovered Carbon Black as a Reinforcing Agent for Ethylene Propylene Diene Rubber Formulation. *Journal of Innovative Science and Engineering*. 10(1), 158-171.

*Corresponding author: Onur YUCAK
E-mail: honour1987@hotmail.com

Keywords:

Recovered carbon black (RCB)
Pyrolysis
Ethylene propylene diene (EPDM) rubber
Waste management
Circular economy

© Copyright 2026 by
Bursa Technical University. Available
online at <http://jise.btu.edu.tr/>



The works published in Journal of Innovative Science and Engineering (JISE) are licensed under a Creative Commons Attribution-NonCommercial 4.0 International License.

ABSTRACT

The environmental risks caused by accumulated rubber wastes have increased the need of recovering these wastes rather than disposing of them. Pyrolysis of waste rubber is recognized as a promising technique. While pyrolysis products oil and gas have previously found industrial applications, there is currently a shortage of viable applications for the solid pyrolysis residue, recovered carbon black (RCB). This study examines the potential use of the RCB as a substitute for virgin carbon black (VCB) in Ethylene Propylene Diene (EPDM) rubber formulation. The goal of this research is to expand technical understanding about the use of the RCB as a green raw material in the rubber industry. In order to characterize the VCB and RCB, Scanning Electron Microscopy (SEM), Energy dispersive X-ray (EDX), Fourier Transform Infrared (FTIR) analyses, and standard test methods were used. The compounds were produced by replacing the VCB with RCB in the EPDM matrix at various loadings. The influence of the RCB addition on the rheological, physical, mechanical and thermal properties of the EPDM composites was evaluated and compared to those formed with the only VCB. The RCB filled compounds usually show detectably inferior properties compared to the only VCB filled compound due to more impurity content, less active surface area, and limited surface functionality of the RCB filler. Although, the VCB can't be completely replaced by the RCB, the results showed that overall performance of the 75-25 compound is better than the reference compound with 100% VCB filler. Moreover, the more RCB may be utilized in combination with the VCB depending on the permissible deviations from the properties of the end products.

1. Introduction

The primary characteristic of elastomers, which gives them their name, is their capacity to experience significant elastic deformations, or to stretch and revert to their initial shape in a reversible manner (Mark et al., 2013). Main constituent of the elastomer

is the rubber. After the rubber, the next most significant part of the elastomer is the fillers. In elastomers, there are two types of fillers: reinforcing and non-reinforcing. While non-reinforcing fillers are preferred to reduce the price, reinforcing ones on the other hand, are used to improve the properties of the elastomers. Due to interactions between the rubber

and the filler surface, the configuration, density, and dynamics of the rubber chains positioned close the surface of the filler have a direct impact on the mechanical and viscoelastic properties of the vulcanizates (Fritzsche & Klüppel, 2010; Morita et al., 2016; Stöckelhuber et al., 2017; Sugimoto et al., 2020).

Carbon black (CB), the second most important and widely used raw material in the rubber industry, is generally used as a reinforcing filler. About 90 % of the world's CB production is used in elastomer applications, and about 70 % alone is used for the production of tires as well as other rubber products for the automotive industry. Additionally, according to yearly volume, carbon black is among the top 50 industrial chemicals worldwide. Global CB production was approximately 12.5 million tons in 2020, and by 2030, it is expected to reach over 17 million tons annually (Ceresana, 2025; Fan et al., 2020; ICBA, 2025). Although global production and demand for CB are increasing, hydrocarbon resources, from which it is produced, in the earth's crust are limited.

With the increase in CB demand, rubber usage, hence the amount of waste generated during production and after use is increasing day by day. Many problems arise as a result of increase in rubber wastes and its irregular storage. Harmful emissions due to combustion, soil pollution in landfills, risk of infectious diseases due to increase in mosquito and insect population near storage areas could be counted among these problems. Legally authorized sanctions for storage and disposal, which is the last step of obtaining waste rubbers, and the threats posed by the accumulated wastes to the environment have increased the importance of recovery of these wastes, rather than their disposal (Adhikari et al., 2000).

As a potential remedy and alternative to current rubber recycling techniques, pyrolysis technology is increasingly attracting the attention of both industry and academia. Rubber waste is thermochemically broken down at temperatures ranging from 400 to 900 °C without oxygen during the pyrolysis process. Depending on the input material and process parameterization, the products are a non-condensable pyrolysis gas (14-46 wt.%), a pyrolysis oil (25-45 wt.%), and a pyrolysis char (25-46 wt.%) (Gao et al., 2022; Martínez et al., 2013; Singh & Ruj, 2016). Accordingly, the demand for natural resources and pollution emissions are reduced when pyrolysis products are employed in other processes, which also improves sustainable economic growth in accordance

with the principles of the circular economy (Winans et al., 2017).

Although the pyrolysis products oil and gas are already being used in industry, there are currently no suitable applications for the solid pyrolysis residue, RCB. There are some studies in the literature to utilize RCB in rubber formulations. Karabork & Tipirdamaz (2016) investigated implementation of RCB, supplied from pyrolysis plant, in new natural rubber (NR) - styrene-butadiene rubber (SBR) blends without any modification. Similarly, Urrego-Yepes et al. (2021) and Jovičić et al. (2023) tested RCB in NR matrix. Martínez et al. (2019) and Vural (2019), produced RCB in laboratory scale pyrolysis unit and after refined it, tested it in SBR matrix. Manjare et al. (2020) investigated the modification of RCB and studied the effect of modified RCB on the properties of NR and SBR vulcanizates. Tian et al. (2021) tried to improve RCB implementation in NR latex matrix by varying mixing processes.

Among the elastomers, ethylene propylene diene monomer (EPDM) is a terpolymer with three components. The structural characteristics of the EPDM elastomer vary depending on the composition of these three components. Because of its saturated main chain, which makes it more resistant to heat, chemicals, UV light, and ozone than many other elastomer kinds, it is one of the most extensively used elastomers (Durmuş Başdemir, 2022). Although, there are various articles in the literature dedicated to explore RCB incorporation in NR and SBR matrixes, there are limited investigations into EPDM, which is the focus of this study. This paper presents a complete characterization of RCB produced in a pyrolysis plant. Furthermore, it examines the substitution of RCB for VCB in a standard EPDM formulation with varying replacement percentages and amounts by preparing compounds using banbury mixer with standard mixing procedures. In light of this, the EPDM composites' rheological performance, density, cross-linking, and thermal behavior were determined. Their typical mechanical characteristics were also identified. In addition, unlike other studies, overall performance of the vulcanizate was evaluated using radar diagrams. The goal of this study is to improve technical understanding of the usage of RCB as a sustainable VCB substitute while taking the circular economy guidelines into account.

2. Material and Methods

2.1. Raw Materials

Dutral Ter 4038 Ep with 60 MU Mooney Viscosity ML 1+4 (125 °C), 27% propylene content and 4,4% ENB content was preferred as an EPDM rubber. Zinc oxide (ZnO) and stearic acid (SA) were used as an activator and procured from Metal Oksit and Vidara firms respectively. Paraffinic oil (PO), supplied from Alkim firm, was utilized as a plasticizer. For accelerator groups in vulcanization chemicals N-Cyclohexyl-2-Mercaptobenzothiazile-sulphenamide (CBS) and Mercaptobenzothiazole (MBT) were used. Sulphur (S-80) was used as a vulcanization agent. EPDM, CBS, MBT and S-80 were procured from Eigenmann company.

N772 semi-reinforcing CB was supplied from OMSK company and used as a VCB for comparison. RCB was supplied from industrial scale pyrolysis plant (Ecosave Co., Turkey). For production of RCB waste tires first pyrolysed in a vertical fixed bed reactor under vacuum atmosphere at 550–600 °C, then pyrolysis char was grinded. No further process was done. In this study, the RCB was used as received condition.

2.2. Characterization of The CBs

In order to characterize VCB and RCB, SEM, EDX analysis, FTIR spectroscopy were used. Moreover, properties including loss on heating, ash content, pour density, pH and Brunauer, Emmett and Teller (BET) surface area were estimated.

SEM images were acquired from the samples coated with a thin gold layer in a vacuum chamber via the sputtering method, using a Carl Zeiss GeminiSEM 300 with Scottky field emission gun at 5 kV acceleration voltage at 100X and 50KX magnifications. In addition, areal EDX analyses were performed at 15 kV acceleration voltage.

For FTIR analysis less than 1% RCB and VCB were mixed with potassium bromide (KBr) to improve energy absorption. Then mixtures were thoroughly crushed using a mortar and pestle and transformed into a thin pellet under a pressure of 10 tones. Prepared samples were analyzed using FTIR (Bruker Vertex V70, USA) spectrometer. Each sample were scanned 64 times at a resolution of 4 cm⁻¹.

Following the ASTM D1506 standard Method A, inorganic material (ash) content was analyzed using muffle furnace (Heraeus M110, Germany). In addition, the loss on heating and the pour density were estimated based on ASTM D1509 and ASTM D1513 standards respectively. Also, the pH values were determined following the ASTM D1512 standard and using a portable pH meter (Hanna HI8314, USA). The BET surface area was measured using nitrogen adsorption instrument (Micromimetrics Tristar II, USA).

2.3. Preparation of Compounds

Compound formulation is based on TS ISO 4097 standard, since ethylene content of EPDM rubber used is higher than 67%, test formulation 2 in the standard was used. Table 1 depicts the formulation of compounds named according to VCB-RCB ratio. All the formulations were given with respect to parts per hundred of rubber (phr). The amounts of EPDM, PO, ZnO, SA, CBS, MBT, and S-80 were the same for all formulations except from type and amount of the CB used.

In this study, all the compounds were made under the same process parameters following TS ISO 4097 Method A3 using 4L laboratory type banbury, and two roll mill (Met-Gür, Türkiye) machines. After preparation of rubber compounds, sufficient material was removed for rheometer tests and the test plates and discs were produced in a compression press with compression production method under 170°C 15 minutes for all the compounds.

Table 1: Rubber formulations.

Raw Materials	100-0	75-25	50-50	25-75	0-100
EPDM	100	100	100	100	100
VCB	100	75	50	25	-
RCB	-	25	50	75	100
ZnO	5	5	5	5	5
SA	1	1	1	1	1
PO	75	75	75	75	75
CBS	3,5	3,5	3,5	3,5	3,5
MBT	1	1	1	1	1
S-80	1,5	1,5	1,5	1,5	1,5

2.4. Dispersion, Rheological, Mechanical and Thermal Properties of The Compounds

In this study, all the samples were prepared and tested following the same processes. Macro-dispersion of CBs in compounds were evaluated using an optical microscope (Dynisco disperGRADER+, USA) in reflection mode under 100X magnification following ASTM D7723 standard. For the test two 6 mm thick compression molded discs were used, five measurements were done and mean of the results determined.

Rheological properties were monitored using a biconical-die roterless curemeters with the sealed-cavity type (Monsanto MDR 2000, USA) at 160 °C for 10 minutes, following the TS ISO 6502-3 standard. Curing parameters; minimum torque (M_L), maximum torque (M_H), ΔM ($M_H - M_L$), scorch time (t_{s2}), curing times (t_{50} and t_{90}) were determined. In addition, the cure rate index (CRI), were calculated from the t_{s2} and t_{90} times by the equation given below.

$$CRI = \frac{100}{t_{90} - t_{s2}} \quad (1)$$

Crosslink density (CLD) of the vulcanized and aged samples were determined using the principle of equilibrium solvent swelling measurements. For each compound both in unaged and aged condition three samples taken from plates were used in the test. First, samples were immersed in toluene (CAS No: 108-88-3) for 72 hours at room temperature. After that the swollen samples were taken out and pat dried quickly with a soft paper towel to remove excess liquid and weighed. Than samples were kept in air-circulating oven at 70 °C for 24 h. At the end, the samples were weighed again. The CLD is calculated by applying a well-known modified Flory–Rehner equation (Flory, 1953).

$$v_e = \frac{-[\ln(1-V_r) + V_r + x_1 V_r^2]}{[V_1(V_r^{1/3} - V_r/2)]} \quad (2)$$

where v_e is the effective number of chains in a real network per unit volume, V_r is the volume fraction of dry rubber, calculated using density of dry rubber (calculated for each sample separately) and solvent (0,8611 g/cm³ for test conditions), and weight of dry rubber and solvent absorbed by sample, V_1 is the molecular volume of solvent (107,00 cm³/mol for test conditions), x_1 is the Flory–Huggins interaction parameter, which can be determined by following equation (Kuei & Gomez, 2016)

$$x_1 = 0,34 + \frac{V_1(\delta_s - \delta_r)^2}{RT} \quad (3)$$

where δ_s is the solubility parameter of solvent (18,2 MPa^{1/2} for toluene), δ_r solubility parameter of polymer (16,3 MPa^{1/2} for EPDM), R is the gas constant (8.314 J/mol), and T is the environmental temperature (299 K) (Fried, 2014; Hrnjak-Murđić et al., 1996; Stelescu et al., 2018). The value of x_1 obtained from the equation is 0,495 and in agreement with previous works (Darko, 2022; Stelescu et al., 2018).

The hardness (H) of samples were measured using electromechanic type Shore A durometer (Gibitre Multiunit Hardness Tester, Italy) following TS ISO 48-4 standard. For testing of H, one 6 mm thick compression molded disc was used, five measurements were done and median of the results determined. Same sample also used in thermal aging and measured after aging. Tensile stress-strain properties were determined according to TS ISO 37 standard at a jaw separation speed of 500 mm/min. using electromechanic type tensile testing machine (Gibitre Tensor Check, Italy) with mechanical extensometer. For tensile testing, ten Type 2 dumbbell specimens were die cut from compression molded square plate having 150 mm side length and 2±0,2 mm thickness. Five of the samples were tested before aging and five of them after aging. At the end of the test, tensile strength at break (S_b), elongation at break (E_b), stress at 50, 100, 200, 300, 400 and 500% (S_{50} , S_{100} , S_{200} , S_{300} , S_{400} and S_{500}) elongations were determined and median of the results reported. Density (D) was determined following Method A of TS ISO 2781 standard using three pieces of rubber taken from plates, having a mass of at least 2,5 g. Density measurements were performed on analytical balance (Sartorius Analytic AC 210 S, Germany) and mean of the results reported.

In order to reveal thermal properties, compression set (CS) and accelerated aging tests were done using cabinet oven with forced air circulation (Heraeus UT6120, Germany). The CS was determined at 70 °C for 22 hours using three samples having 29±0,5 mm diameter and 12,5±0,5 mm thickness in accordance with TS ISO 815-1 standard Method A. Median of the CS of the three samples reported. Thermal aging tests were performed on hardness and tensile test specimens at 100 °C for 70 hours following TS ISO 188 standard. In addition, for CLD determinations after aging, samples taken from plates were also aged at same aging conditions.

3. Results and Discussion

3.1. Characterization of The CBs

Figure 1 represents the SEM image of the VCB and RCB samples. As can be seen in SEM images each CB particle is fused together by covalent bonds and

formed aggregates. While SEM image of RCB shows the many structure of the aggregations, the VCB SEM image shows very few aggregations. In addition, particle size distribution is wider in the RCB in comparison to the VCB. On the other hand, SEM pictures taken at 50KX magnification are almost identical for both VCB and RCB.

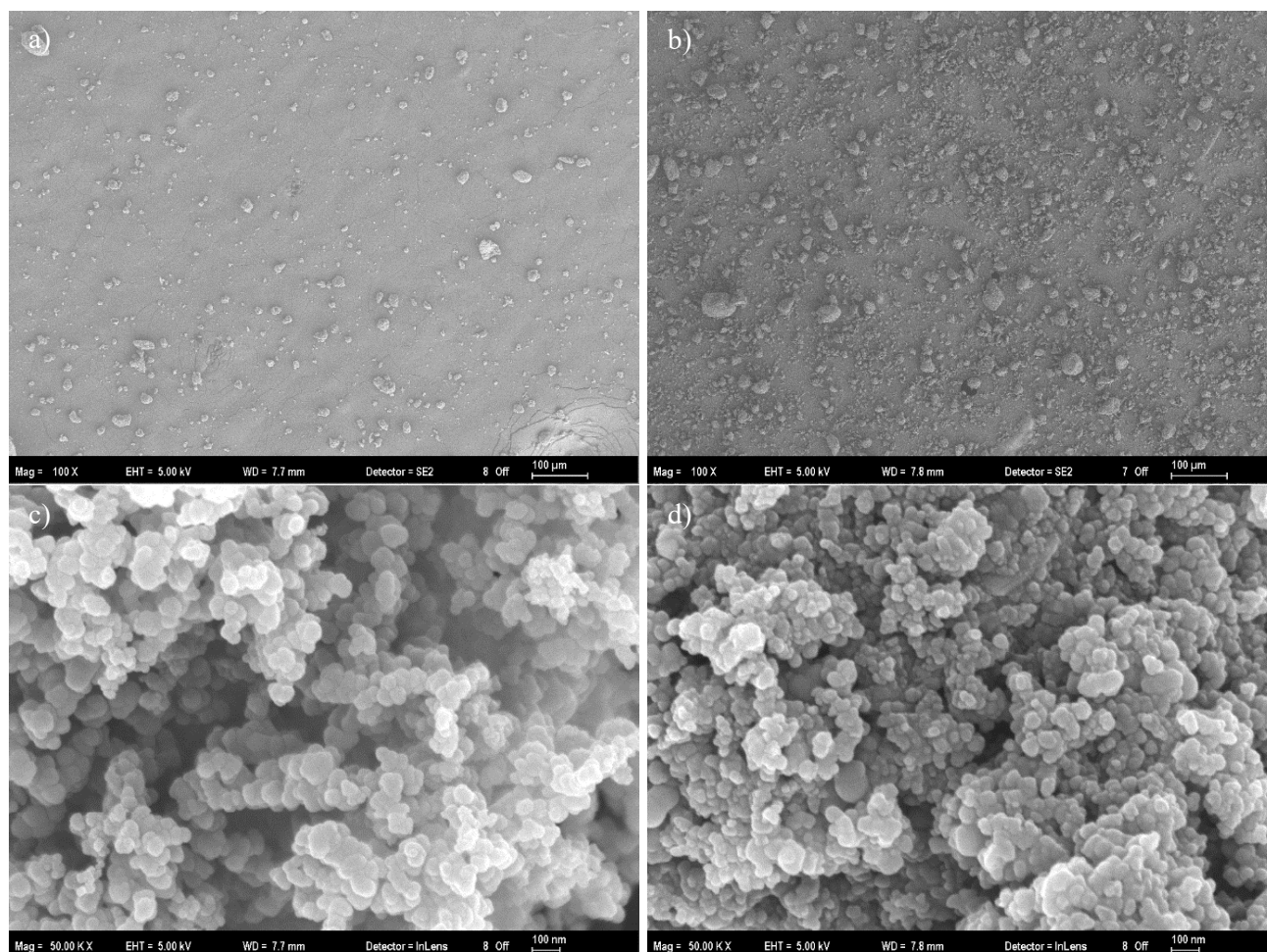


Figure 1. At 100X magnification SEM image of a) VCB, b) RCB; at 50KX magnification SEM image of c) VCB, d) RCB.

Table 2: EDX analysis results.

Element	VCB		RCB	
	Weight %	Atomic %	Weight %	Atomic %
C	98,37	99,38	83,53	90,33
O	-	-	7,17	5,82
Si	-	-	4,04	1,87
S	1,63	0,62	3,54	1,44
Zn	-	-	0,95	0,19
Al	-	-	0,41	0,20
Na	-	-	0,18	0,10
Ca	-	-	0,18	0,06

The elements present in RCB and VCB, detected by EDX analysis, are listed in Table 2. The analysis shows that RCB and VCB contain carbon (C) and

sulphur (S), but apart from that: oxygen (O), silicon (Si), and zinc (Zn) are also present in the RCB as a major element, having weight % of: 7,17, 4,04 and

0,95 respectively. Si and Zn in the RCB is associated with silica (SiO_2) and ZnO present in waste rubber formulation. The higher O content in RCB can be related to SiO_2 , ZnO and oxidation that may occur on the carbonaceous surface of RCB at higher pyrolysis temperature (Darmstadt et al., 1995). As a result, the RCB employed in this investigation has impurities that may have an impact on its cure kinetics and final mechanical characteristics.

Figure 2 illustrates the FTIR spectra of both VCB and RCB. Although they showed similarities, they also exhibited important differences in terms of existence and intensity of peaks and bands. In both spectra, peaks around 2920 cm^{-1} and 2845 cm^{-1} indicate the asymmetric and symmetric C-H stretching of aliphatic structures (Fanning & Vannice, 1993; Khelifi et al., 2010), the peaks in the range of $2250\text{--}2400\text{ cm}^{-1}$ indicate C=C stretching of alkynes (Tran et al., 2017) and the peak at 461 cm^{-1} indicates S-S stretching (Colom et al., 2016). Moreover, for RCB peaks seen at 1092 cm^{-1} and 797 cm^{-1} belong to SiO_2 (Miller & Wilkins, 1952), and the peaks at 1555 cm^{-1} and 1449 cm^{-1} belong to ZnO (Colom et al., 2009), which coincide with EDX results of RCB. On the other hand, in VCB peak appeared at 1630 cm^{-1} is attributed to C=O stretching, which suggests the presence of carboxyl, ketenes (Fanning & Vannice,

1993), lactones (Tangsathitkulchai, Ngernyen, & Tangsathitkulchai, 2009; Xiao & Thomas, 2004), and pyrones (Barroso-Bogeat et al., 2014). The peak at 1470 cm^{-1} is attributed to the asymmetric stretching of sulfates (Smith, 2018) and/or alkane groups as a result of C=C stretching (Pretsch et al., 2009). Absence of these peaks for the RCB show that these functional groups have been lost throughout the recovery process.

Loss on heating, ash content, bulk density, pH test and BET analysis results are summarized in Table 3. Loss on heating and ash content of samples are related with moisture and inorganic material content respectively. Both values are higher for RCB than VCB as expected. Ash content test results also coincide with EDX results. Pour density values are also different, which can be attributed to difference in filler structure and size, and ash content, as evident from the SEM and EDX analyses. From the pH values obtained, VCB and RCB have basic and neutral character respectively. While basic character can be attributed to functional groups present on the surface, neutral character on the other hand is related with absence of functional groups, which was confirmed in FTIR analysis. BET surface area values obtained are in line with the SEM image analysis results.

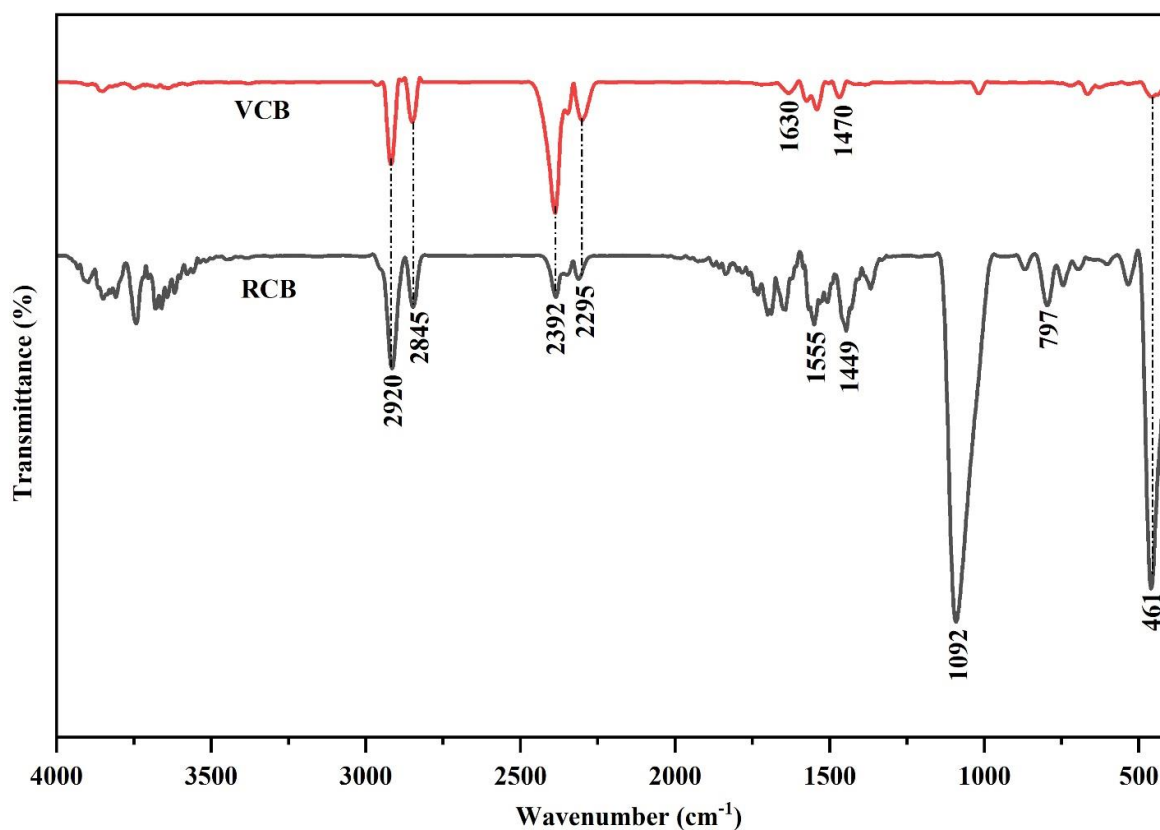


Figure 2. FTIR spectra of VCB and RCB.

Table 3: Properties of the VCB and RCB.

Property	Loss on heating, %	Ash content, %	Pour density, kg/m ³	pH value	BET surface area, m ² /g
VCB	0,03	0,53	494	9,65	35,7
RCB	0,42	16,63	424	7,05	11,2

3.2. Dispersion, Rheological and CLD Properties of The Compounds

Macro-dispersion properties of the EPDM vulcanizates are given in Table 4 with their standard deviations. In addition, weight fraction of CB, calculated from rubber formulations given in Table 1 and ash content in Table 3, and volume fraction of the CB, required to calculate percent dispersion of CB, calculated from the weight fractions, in the compounds are also given in Table 4. In compound preparation it is aimed to reduce average CB agglomerate size by breaking van der Waals Forces, when this disintegration is not sufficient, agglomerates form irregular dispersion in mixtures (Özkan, 2008). It can be inferred from the Table 4 that as the RCB to VCB ratio increased; percent white area (the portion of the scan area which contains

bumps, or other surface defects) and average agglomerate size increased, but percent dispersion of CBs in the compounds decreased. Although all the compounds were prepared using same process parameters, fraction of undispersed filler in the 100-0, 75-25 and 50-50 compounds is nearly 0, 4, 10% respectively, on the other hand, for the 25-75 and 0-100 compounds is above 25 and 50% respectively. The RCB was obtained from waste rubber pyrolysis and composed of mixture of different types of CBs, and ash, hence increase in amount of RCB caused increase in amount of undispersed filler due to increase in the average agglomerate size and size distribution. Furthermore, D of the compounds is also given in Table 4 with their standard deviations. As the amount of RCB in the compound increased, the D of the compounds decreased, which is a direct consequence of decrease in total CB present in compounds and dispersion fraction of it.

Table 4: CB dispersion properties of the compounds.

Property	100-0	75-25	50-50	25-75	0-100
Calculated weight fraction of CB (%)	34,84	33,39	31,94	30,49	29,05
Calculated volume fraction of CB (%)	21,17	20,77	20,12	19,69	19,16
White area (%)	0,27 ± 0,09	2,68 ± 0,13	5,97 ± 0,46	11,51 ± 0,67	18,14 ± 0,72
Average agglomerate size (µm)	9,64 ± 5,67	11,99 ± 7,32	12,87 ± 7,70	14,27 ± 8,41	16,54 ± 10,04
Dispersion (%)	99,85 ± 0,07	96,01 ± 0,49	89,45 ± 1,07	74,94 ± 3,01	43,99 ± 3,38
D (g/cm ³)	1,094 ± 0,001	1,089 ± 0,002	1,071 ± 0,001	1,064 ± 0,001	1,051 ± 0,000

Understanding the curing properties of elastomeric materials is critical when selecting the raw material composition in order to achieve proper component mixing and separate the final product from the mold while ensuring that all production process steps follow energy-saving guidelines and environmental regulations (Kojić et al., 2018). The rheological properties of vulcanizates, at 160°C, i.e.: M_L, M_H, ΔM, t_{s2}, t₅₀, t₉₀ and CRI are listed in Table 5.

The physical filler-filler and filler-rubber interactions in the system prior to the curing process determine M_L, which is an indirect indicator of the viscosity of the compound (Jovičić et al., 2022). As illustrated in Table 5, the M_L of only VCB filled EPDM is 0,48

lb.in and decreased to 0,44 and 0,34 lb.in for 75-25, 50-50 compounds respectively. For the other compounds as the RCB loading of compound increased, M_L remained almost same. In the unvulcanized system, the filler-filler and filler-rubber physical interactions diminish as amount of RCB rises, which can be explained by formation of carbonaceous residue on the RCB surface due to polymer degradation during pyrolysis. Carbonaceous residue deposits enclose the empty space between the RCB aggregate's primary particles, obstructing an active area of surfaces (Darmstadt et al., 2000).

As can be seen in the Table 5, the M_H and ΔM values first increased and reached highest values for the 75-

25 compound and decreased as the RCB to VCB ratio increased. Opposite trend can be seen for t_{s2} and t_{50} times, i.e.; the values first decreased and became lowest up to 25 phr RCB content and then increased. From the elemental analysis of CBs, we know that RCB contains more S than VCB, therefore increase in M_H and ΔM , and decrease in t_{s2} and t_{50} times for 75-25 compound can be attributed to increase in S content. Lower the surface area of filler, lower the physical adsorption of rubbers by the filler (Manoj et al., 2011; M. J. Wang, 1998). Dispersion analysis results reveal that as the VCB was replaced by RCB in the compounds, average agglomerate size increased, hence the surface area of agglomerates became lower. This explains why further increase in RCB content ended up with opposite trend in curing characteristics, although amount of S present in the compounds increase.

The optimum curing time, t_{90} is 6,80 minutes for the only VCB loaded system and increased up to 8,25 minutes as the VCB is replaced by RCB. The CRI value is the highest for 100-0 compound and decreases gradually as the RCB to VCB ratio increased in the system. As the filler loading increases, t_{90} decreases, hence CRI increases (Jovanović et al., 2009; Morton, 1999). As can be seen in Table 4, as the RCB content of compound increased, filler dispersion and total filler fraction decreased. Therefore, decrease in t_{90} time and CRI can be attributed to these findings.

Polymers' ability to swell is typically governed by their CLDs; the lower the density of the chain network, the more solvent molecules they can hold. Higher CLD, on the other hand, inhibits the absorption of solvent molecules into the networks and reduces the gaps between the chains by making the polymer chains difficult to stretch (Bajpai & Giri, 2003; Shafee & Naguib, 2003; Valentin et al., 2008). The values of the CLD, for the compounds both in unaged and aged conditions, are given in Table 6 with their standard deviations. As can be seen in Table 6, the CLD is higher for sample containing only VCB and as the VCB replaced by RCB, the CLD decreased. Decrease in the CLD can be explained by the absence of functional groups in RCB, the size and structure of RCB, which reduces its active surface area, amount of undispersed filler and the presence of lower CBs, i.e., as the RCB content in the compound increases, amount of CB decreases due to inorganic substances present in it.

As can be seen in Table 6, after thermal aging CLD of the compounds increased. During aging process while formation of new crosslinks causes increase in the CLD, disintegration of existing crosslinks decreases the CLD (Choi et al., 2008). Therefore, improvement of the CLD by the thermal aging implies that formation of new crosslinks prevails over disintegration of the preexisting crosslinks.

Table 5: Rheological properties of the compounds.

Property	100-0	75-25	50-50	25-75	0-100
M_L (lb.in)	0,48	0,44	0,34	0,34	0,36
M_H (lb.in)	6,96	7,65	6,68	5,94	5,52
ΔM (lb.in)	6,48	7,21	6,34	5,60	5,16
t_{s2} (min)	4,38	4,12	4,60	4,77	4,43
t_{50} (min)	5,02	4,75	5,18	5,23	4,83
t_{90} (min)	6,80	7,22	8,03	8,25	8,15
CRI (min^{-1})	41,38	32,26	29,13	28,71	26,91

Table 6: CLD of the compounds before and after aging.

CLD (10^{-4} mol/cm^3)	100-0	75-25	50-50	25-75	0-100
Before aging	$2,396 \pm 0,013$	$1,784 \pm 0,015$	$1,299 \pm 0,015$	$1,057 \pm 0,004$	$0,818 \pm 0,008$
After aging	$2,780 \pm 0,006$	$2,021 \pm 0,054$	$1,558 \pm 0,031$	$1,277 \pm 0,012$	$0,904 \pm 0,008$

3.3. Mechanical Properties

Rubber reinforcement is the result of physical and chemical interactions between the rubber and the reinforcing filler. The effects of substituting RCB for VCB in EPDM compounds on the sample H are shown in Table 7 with their standard deviations. The

H varied with changes in the ratios of the VCB and RCB in the system. The H decreased from 50 to 42 Shore A as the amount of RCB content was increased. The tensile stress-strain properties of compounds are also given in Table 7 with their standard deviations. A drop in the S_b from 12,8 to 9,4 MPa was observed as the RCB content of the compound was increased.

For the 100-0 compound the E_b observed, was 535% and for the 0-100 compound raised to 642%. Moreover, as evident from Table 7, as the amount of the RCB loading in the system increased, values of the S_{50} , S_{100} , S_{200} , S_{300} , S_{400} and S_{500} decreased.

Change in the mechanical properties can be attributed to several factors. First of all, dispersion analysis has shown that average agglomerate size increased as the RCB content increased in the vulcanizate. As particle size increases or surface area becomes smaller, the degree of entanglement between filler and rubber lessens, hence stress transfer from the matrix to the fillers is less effective (Litvinov & Steeman, 1999; Li et al., 2008; Manoj et al., 2011; M. J. Wang, 1998). The surface area is just one factor that influences the reinforcing characteristics of CB in the compounds. Another factor is dispersion of filler in the compounds. As the amount of undispersed filler

increase, the mechanical properties get worse (Özkan, 2008). Variation in the mechanical properties is not due only to surface area and dispersion parameter but is also due to the surface functional groups on CB. From the pH and FTIR analyses results, it can be speculated that lack of these functional groups on RCB induced slightly weaker interactions with the EPDM matrix where the resulting compounds exhibited lower mechanical properties than the compound including only VCB. Finally, ash content of the RCB is another factor effecting the mechanical properties. As the RCB content increased, amount of inorganic materials increased, hence amount of reinforcing filler in the compound decreased. As seen in Table 6, all the factors mentioned above decreased the CLD, which is in turn caused decrease in H , S_b , S_{50} , S_{100} , S_{200} , S_{300} , S_{400} and S_{500} values and increase in E_b of the compounds.

Table 7: Mechanical properties of the compounds.

Property	100-0	75-25	50-50	25-75	0-100
H (Shore A)	50 ± 0,7	50 ± 0,9	45 ± 0,5	42 ± 0,7	42 ± 0,5
S_b (MPa)	12,8 ± 0,6	12,1 ± 0,5	11,8 ± 0,5	10,0 ± 0,3	9,4 ± 0,5
E_b (%)	535 ± 20	579 ± 8	626 ± 30	612 ± 34	642 ± 42
S_{50} (MPa)	0,92 ± 0,09	0,78 ± 0,04	0,62 ± 0,08	0,53 ± 0,07	0,57 ± 0,10
S_{100} (MPa)	1,59 ± 0,10	1,13 ± 0,05	0,87 ± 0,09	0,77 ± 0,08	0,77 ± 0,10
S_{200} (MPa)	3,23 ± 0,11	1,95 ± 0,05	1,31 ± 0,11	1,08 ± 0,09	1,00 ± 0,07
S_{300} (MPa)	4,73 ± 0,16	2,76 ± 0,05	1,67 ± 0,06	1,34 ± 0,09	1,23 ± 0,09
S_{400} (MPa)	6,81 ± 0,36	3,78 ± 0,08	2,26 ± 0,11	1,82 ± 0,20	1,55 ± 0,14
S_{500} (MPa)	10,63 ± 0,98	6,26 ± 0,28	3,52 ± 0,58	2,98 ± 0,94	2,31 ± 0,45

3.4. Thermal Properties

Figure 3 shows values of S_b and E_b both before and after aging with corresponding change, in bar charts with their standard deviations. After the thermal aging process, there was no change in the S_b of the compound loaded with only RCB. The highest change recorded is -9% for 100-0 compound. A decrease was also recorded for 50-50 and 25-75 compounds, while an increase was observed only in the 75-25 compound and its value is 2%. The S_b of a compound increases with increasing CLD until it reaches a critical density, beyond this point, the S_b decreases due to reduced energy dissipation through molecular mobility (Pimolsiriphol et al., 2007). Therefore, although the CLD of the compounds increased after aging, changes in the S_b are not parallel with this increase. On the other hand, the E_b decreased slightly from 642% to 596% for the 0-100 compound. Similar trend was followed for the other compounds. The highest decrease recorded is 11% for 100-0 compound. Elastomeric materials may undergo

chain scission, degradation, and cross-linking events during aging. (Z. Wang et al., 2016). For the EPDM compounds, the CLD increased after the aging, as presented in Table 6, which is the main cause of decrease in the E_b after aging.

Figure 4 illustrates how the ratio of VCB to RCB affects the H after heat aging and the CS, in bar charts with their standard deviations. The H of the compounds rose as the RCB content increased. The increase in the H after aging can be attributed to increase in the CLD as in the E_b . CS is a measure of deformation remaining after release of the compressive force. There is no direct relationship was found between filler loading and the CS. However, value of the CS is a bit lower for compound containing only VCB, than other compounds. 100-0 sample has the lowest CS (13%) whereas those of samples filled with 50 and 100% RCB are in the middle position (16% and 15% respectively). 75-25 and 25-75 samples have the highest CS (both are 17%). Similar finding was reported in literature (Urrego-Yepes et al., 2021).

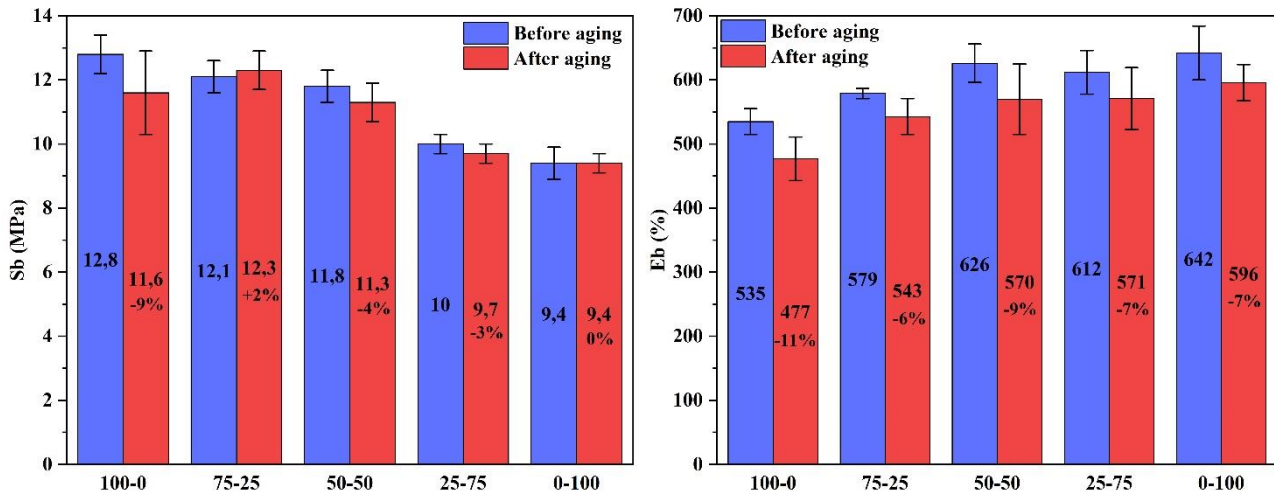


Figure 3. Change in S_b and E_b of the compounds after aging.

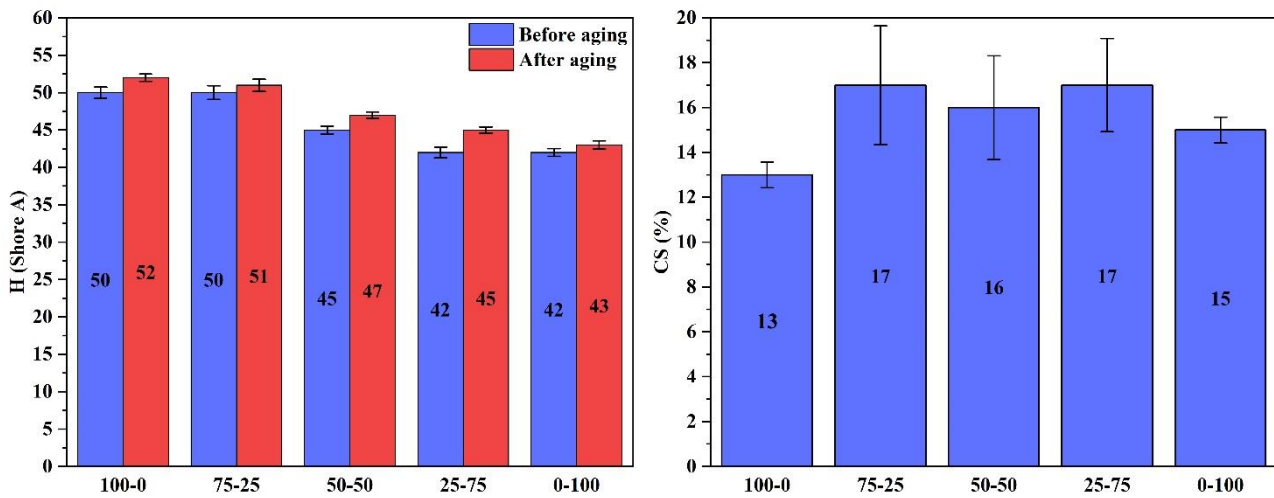


Figure 4. Change in H after aging, and CS of the compounds.

4. Conclusion

In this study, utilization of RCB as a reinforcing agent in EPDM formulations have been studied. After examining the characteristics of each filler, detailed evaluations were performed to better understand the effects of these fillers on the physical, mechanical, and thermal properties of EPDM rubber. Due to the higher inorganic material content, higher average agglomerate size and uneven size distribution, and limited surface functionality, utilization of the RCB resulted in somewhat poor interactions across the EPDM matrix. As the RCB content in the compounds increased, D, H, and S_b decreased, E_b increased. After thermal aging, 75-25 compound shows better performance in terms of change in S_b , E_b and H, since change in properties with respect to properties before aging are less than other compounds.

In order to better evaluate overall performance of compounds, values of S_b , E_b , H, D (12,8 MPa, 535%, 50 Shore A, 1,094 g/cm³ respectively) and CS (since

CS is a permanent deformation, hence negative property, nonpermanent deformation values were used, which is 87 for 100-0 compound, and 83, 84, 83, 85 for other compounds respectively) of the compound containing only VCB were accepted as 100%. S_b , E_b , H, D and CS values of other compounds and values of S_b , E_b and H after thermal aging for all the compounds were determined with respect to reference values. Results were given using radar diagrams in Figure 5. As can be seen in Figure 5, overall properties of the compound with only RCB are not good as reference compound. However, the 75-25 compound outperformed the 100-0, since in the radar diagram shape of the filling is closer to a regular octagon, i.e, values are closer to 100%. Furthermore, the more RCB may be used in combination with VCB depending on the acceptable deviations from the properties of the final products, as such, for 20% deviation from the original properties up to 50% RCB can be used as a filler. Consequently, the RCB and VCB can be used together. These findings are expected to advance technical knowledge on the use

of RCB as a long-term alternative for VCB in the rubber sector.

It still seems like a good idea to replace VCB in compounds with RCB, given the growing global demand for CB and the limited supply of fossil fuels utilized for this purpose. Further investigations can be conducted, for instance, after purifying, milling, and classifying the RCB based on agglomerate size using screening, or functionalizing the RCB surface. In

addition, to compensate decrease in filler content due to impurities, CB phr in the rubber formulation can be increased. Moreover, preparation methods can be changed to improve CB dispersion. Apart from stated suggestions, additives can be used to enhance overall properties. This study is only the beginning of our research, we are planning to use nano additives to improve RCB utilization in EPDM compounds in the future research.

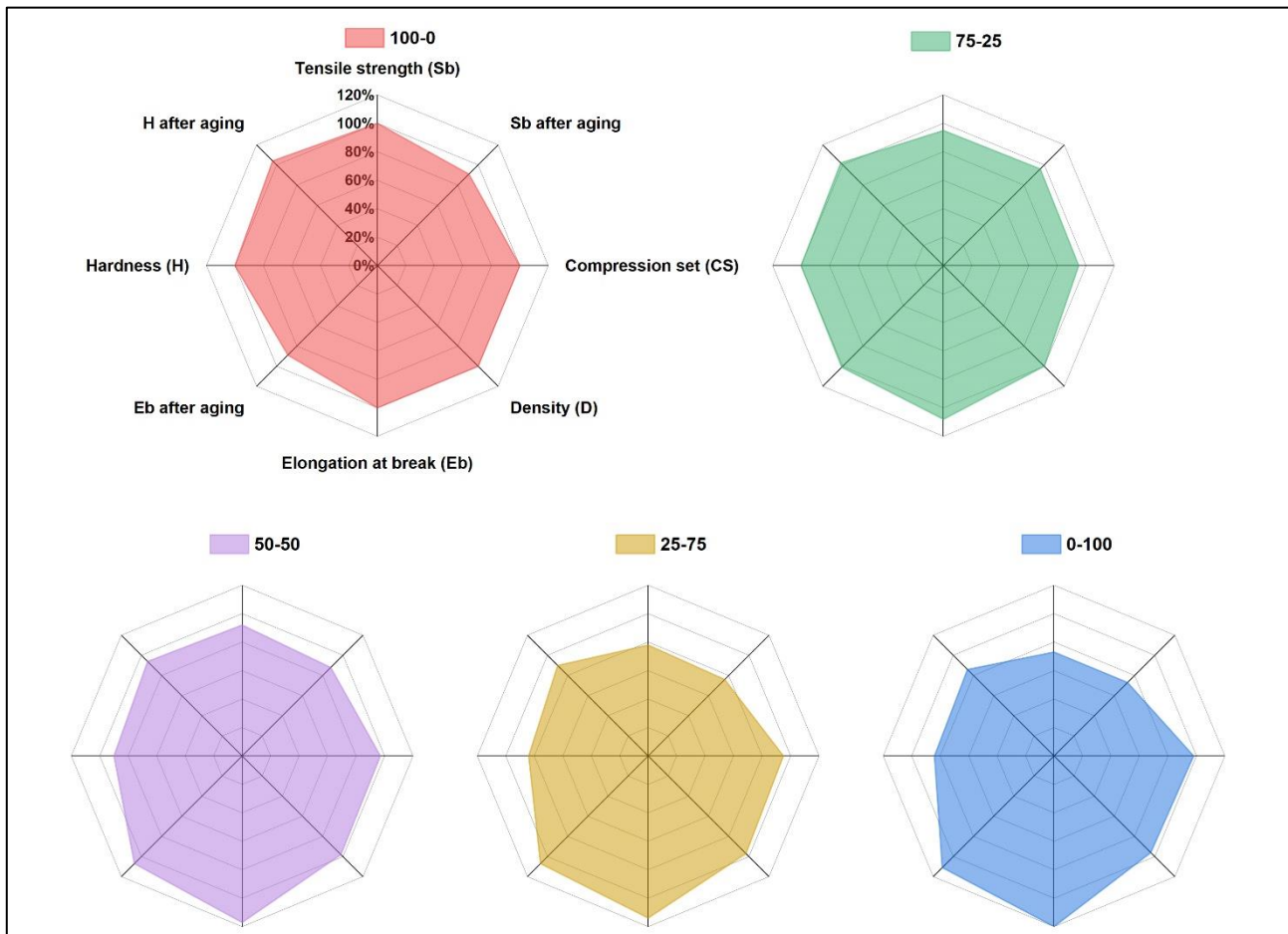


Figure 5. Overall comparison of properties of the compounds with respect to the 100-0 compound.

Article Information

Financial Disclosure: This study was carried out within the scope of Bursa Technical University Scientific Research Projects Coordinatorship (BTU BAP) Research Project 230D006. We gratefully acknowledge the financial support provided by BTU BAP. Also, we would like to thank Treco Kauçuk ve Kimyasalları San. ve Tic. Ltd. Şti. for providing production support to this study.

Authors' Contribution: Concept: Y.O.; Design: Y.O.; Supervision: U.D., H.H.L.; Resources: Y.O.; Data Collection: Y.O.; Analysis: Y.O.; Literature

Search: Y.O.; Writing Manuscript: Y.O.; Critical Review: Y.O., U.D., H.H.L.

Conflict of Interest/Common Interest: No conflict of interest or common interest has been declared by the authors.

Ethics Committee Approval: This study does not require ethics committee permission or any special permission.

Artificial Intelligence Statement: The author(s) bear full responsibility for the content and accuracy of their work, including any use of artificial intelligence (AI) technologies, and confirm that they have read the AI Policy, which is accessible on the journal's website.

References

- Adhikari, B., De, D., & Maiti, S. (2000). Reclamation and recycling of waste rubber. *Progress in Polymer Science*, 25(7), 909–948.
- Bajpai, A. K., & Giri, A. (2003). Water sorption behaviour of highly swelling (carboxy methylcellulose-g-polyacrylamide) hydrogels and release of potassium nitrate as agrochemical. *Carbohydrate Polymers*, 53(3), 271–279.
- Barroso-Bogeat, A., Alexandre-Franco, M., Fernández-González, C., & Gómez-Serrano, V. (2014). FT-IR Analysis of Pyrone and Chromene Structures in Activated Carbon. *Energy and Fuels*, 28(6), 4096–4103.
- Ceresana. (2022). *Carbon Black Market Report: Global Industry Analysis, 2030*. <https://ceresana.com/en/produkt/carbon-black-market-report> (Accessed: 8 March 2025)
- Choi, S. S., Kim, J. C., Lee, S. G., & Joo, Y. L. (2008). Influence of the cure systems on long time thermal aging behaviors of NR composites. *Macromolecular Research*, 16(6), 561–566.
- Colom, X., Andreu-Mateu, F., Cañavate, F. J., Mujal, R., & Carrillo, F. (2009). Study of the influence of IPPD on thermo-oxidation process of elastomeric hose. *Journal of Applied Polymer Science*, 114(4), 2011–2018.
- Colom, X., Faliq, A., Formela, K., & Cañavate, J. (2016). FTIR spectroscopic and thermogravimetric characterization of ground tyre rubber devulcanized by microwave treatment. *Polymer Testing*, 52, 200–208.
- Darko, C. (2022). The link between swelling ratios and physical properties of EPDM rubber compound having different oil amounts. *Journal of Polymer Research*, 29(8), 1–10.
- Darmstadt, H., Roy, C., & Kaliaguine, S. (1995). Characterization of pyrolytic carbon blacks from commercial tire pyrolysis plants. *Carbon*, 33(10), 1449–1455.
- Darmstadt, H., Roy, C., Kaliaguine, S., Xu, G., Auger, M., Tuel, A., & Ramaswamy, V. (2000). Solid state ¹³C-NMR spectroscopy and XRD studies of commercial and pyrolytic carbon blacks. *Carbon*, 38(9), 1279–1287.
- Durmuş Başdemir, Y. (2022). *Effect of carbon black type and vulcanization system on static and dynamic mechanical properties of new generation ethylene propylene diene monomer (EPDM) elastomers*. [Doctoral dissertation, Hacettepe University]. YÖK National Thesis Center.
- Fanning, P. E., & Vannice, M. A. (1993). A DRIFTS study of the formation of surface groups on carbon by oxidation. *Carbon*, 31(5), 721–730.
- Fan, Y., Fowler, G. D., & Zhao, M. (2020). The past, present and future of carbon black as a rubber reinforcing filler – A review. *Journal of Cleaner Production*, 247, 119115.
- Flory, P. J. (1953). *Principles of Polymer Chemistry*. Cornell University Press.
- Fried, J. R. (2014). *Polymer Science & Technology*. Pearson.
- Fritzsche, J., & Klüppel, M. (2010). Structural dynamics and interfacial properties of filler-reinforced elastomers. *Journal of Physics: Condensed Matter*, 23(3), 035104.
- Gao, N., Wang, F., Quan, C., Santamaria, L., Lopez, G., & Williams, P. T. (2022). Tire pyrolysis char: Processes, properties, upgrading and applications. *Progress in Energy and Combustion Science*, 93, 101022.
- Hrnjak-Murđić, Z., Jelenčić, J., & Bravar, M. (1996). The role of molar volume of the organic solvents in the swelling system EPDM vulcanizate/solvent. *Die Angewandte Makromolekulare Chemie*, 242(1), 85–96.
- ICBA. (n.d.). *What is Carbon Black?* <https://www.carbon-black.org/new-page-2> (Accessed: 8 March 2025)
- Jovanović, V., Budinski-Simendić, J., Samardžija-Jovanović, S., Marković, G., Marinović-Cincović, M., & Budinski-Simendić, J. (2009). The influence

- of carbon black on curing kinetics and thermal aging of acrylonitrile-butadiene rubber. *Chemical Industry & Chemical Engineering Quarterly*, 15(4), 283–289.
- Jovičić, M., Bera, O., Stojanov, S., Pavličević, J., Govedarica, D., Bobinac, I., & Hollo, B. B. (2023). Effects of recycled carbon black generated from waste rubber on the curing process and properties of new natural rubber composites. *Polymer Bulletin*, 80(5), 5047–5069.
- Karabork, F., & Tipirdamaz, S. T. (2016). Influence of pyrolytic carbon black and pyrolytic oil made from used tires on the curing and (dynamic) mechanical properties of natural rubber (NR)/styrene-butadiene rubber (SBR) blends. *Express Polymer Letters*, 10(1), 72–82.
- Khelifi, A., Almazán-Almazán, M. C., Pérez-Mendoza, M., Domingo-García, M., López-Domingo, F. J., Temdrara, L., López-Garzón, F. J., & Addoun, A. (2010). Influence of nitric acid concentration on the characteristics of active carbons obtained from a mineral coal. *Fuel Processing Technology*, 91(10), 1338–1344.
- Kojić, D., Lazić, N., Budinski-Simendić, J., Špirkova, M., Dugić, P., Ostojić, S., & Pavličević, J. (2018). The influence of combined active fillers on the properties of elastomeric materials for eco-friendly tyres. *Hemijaska Industrija*, 72(5), 293–303.
- Kuei, B., & Gomez, E. D. (2016). Chain conformations and phase behavior of conjugated polymers. *Soft Matter*, 13(1), 49–67.
- Litvinov, V. M., & Steeman, P. A. M. (1999). EPDM–Carbon Black Interactions and the Reinforcement Mechanisms, As Studied by Low-Resolution 1H NMR. *Macromolecules*, 32(25), 8476–8490.
- Li, Z. H., Zhang, J., & Chen, S. J. (2008). Effects of carbon blacks with various structures on vulcanization and reinforcement of filled ethylene-propylene-diene rubber. *Express Polymer Letters*, 2(10), 695–704.
- Manjare, S., Dwivedi, C., & Rajan, S. K. (2020). Recycling of waste tire by pyrolysis to recover carbon black: Alternative & environment-friendly reinforcing filler for natural rubber compounds. *Composites Part B: Engineering*, 200, 108346.
- Manoj, K. C., Kumari, P., & Unnikrishnan, G. (2011). Cure characteristics, swelling behaviors, and mechanical properties of carbon black filler reinforced EPDM/NBR blend system. *Journal of Applied Polymer Science*, 120(5), 2654–2662.
- Mark, J. E., Erman, B., & Roland, C. M. (2013). The Science and Technology of Rubber, Fourth Edition. *The Science and Technology of Rubber, Fourth Edition*, 1–786.
- Martínez, J. D., Cardona-Urbe, N., Murillo, R., García, T., & López, J. M. (2019). Carbon black recovery from waste tire pyrolysis by demineralization: Production and application in rubber compounding. *Waste Management*, 85, 574–584.
- Martínez, J. D., Puy, N., Murillo, R., García, T., Navarro, M. V., & Mastral, A. M. (2013). Waste tyre pyrolysis – A review. *Renewable and Sustainable Energy Reviews*, 23, 179–213.
- Miller, F. A., & Wilkins, C. H. (1952). Infrared Spectra and Characteristic Frequencies of Inorganic Ions. *Analytical Chemistry*, 24(8), 1253–1294.
- Morita, H., Toda, M., & Honda, T. (2016). Analysis of the end-segment distribution of a polymer at the interface of filler-filled material. *Polymer Journal* 2016 48:4, 48(4), 451–455.
- Morton, M. (1999). *Rubber Technology*. Springer Science+Business Media Dordrecht.
- Özkan, F. (2008). Kauçukta Dağılım ve Önemi. *Kauçuk*, 32, 20–22.
- Pimolsiriphol, V., Saeoui, P., & Sirisinha, C. (2007). Relationship Among Thermal Ageing Degradation, Dynamic Properties, Cure Systems, and Antioxidants in Natural Rubber Vulcanisates. *Polymer-Plastics Technology and Engineering*, 46(2), 113–121.
- Pretsch, E., Bühlmann, P., & Badertscher, M. (2009). *Structure Determination of Organic Compounds: Tables of Spectral Data*. Springer
- Shafee, E. El, & Naguib, H. F. (2003). Water sorption in cross-linked poly(vinyl alcohol) networks. *Polymer*, 44(5), 1647–1653.
- Singh, R. K., & Ruj, B. (2016). Time and temperature depended fuel gas generation from pyrolysis of real world municipal plastic waste. *Fuel*, 174, 164–171.

- Smith, B. (2018). *Infrared spectral interpretation: a systematic approach*. CRC Press
- Stelescu, M. D., Airinei, A., Manaila, E., Craciun, G., Fifere, N., Varganici, C., Pamfil, D., & Doroftei, F. (2018). Effects of Electron Beam Irradiation on the Mechanical, Thermal, and Surface Properties of Some EPDM/Butyl Rubber Composites. *Polymers* 2018, Vol. 10, Page 1206, 10(11), 1206.
- Stöckelhuber, K. W., Wießner, S., Das, A., & Heinrich, G. (2017). Filler flocculation in polymers – a simplified model derived from thermodynamics and game theory. *Soft Matter*, 13(20), 3701–3709.
- Sugimoto, S., Inutsuka, M., Kawaguchi, D., & Tanaka, K. (2020). The effect of interfacial dynamics on the bulk mechanical properties of rubber composites. *Polymer Journal*, 52(2), 217–223.
- Tangsathitkulchai, C., Ngernyen, Y., & Tangsathitkulchai, M. (2009). Surface modification and adsorption of eucalyptus wood-based activated carbons: Effects of oxidation treatment, carbon porous structure and activation method. *Korean Journal of Chemical Engineering*, 26(5), 1341–1352.
- Tian, X., Zhuang, Q., Han, S., Li, S., Liu, H., Li, L., Zhang, J., Wang, C., & Bian, H. (2021). A novel approach of reapplication of carbon black recovered from waste tyre pyrolysis to rubber composites. *Journal of Cleaner Production*, 280, 124460.
- Tran, H. N., Huang, F. C., Lee, C. K., & Chao, H. P. (2017). Activated carbon derived from spherical hydrochar functionalized with triethylenetetramine: Synthesis, characterizations, and adsorption application. *Green Processing and Synthesis*, 6(6), 565–576.
- Urrego-Yepes, W., Cardona-Urbe, N., Vargas-Isaza, C. A., & Martínez, J. D. (2021). Incorporating the recovered carbon black produced in an industrial-scale waste tire pyrolysis plant into a natural rubber formulation. *Journal of Environmental Management*, 287, 112292.
- Valentín, J. L., Carretero-González, J., Mora-Barrantes, I., Chassé, W., & Saalwächter, K. (2008). Uncertainties in the determination of cross-link density by equilibrium swelling experiments in natural rubber. *Macromolecules*, 41(13), 4717–4729.
- Vural, U. S. (2019). Pirolitik Karbon Siyahının Rafinasyonu Ve Kauçuk Sektöründe Kullanımı. *Afyon Kocatepe Üniversitesi Fen Ve Mühendislik Bilimleri Dergisi*, 19(3), 850–860.
- Wang, M. J. (1998). Effect of Polymer-Filler and Filler-Filler Interactions on Dynamic Properties of Filled Vulcanizates. *Rubber Chemistry and Technology*, 71(3), 520–589.
- Wang, Z., Zhang, X., Wang, F., Lan, X., & Zhou, Y. (2016). Effects of aging on the structural, mechanical, and thermal properties of the silicone rubber current transformer insulation bushing for a 500 kV substation. *SpringerPlus*, 5(1), 1–6.
- Winans, K., Kendall, A., & Deng, H. (2017). The history and current applications of the circular economy concept. *Renewable and Sustainable Energy Reviews*, 68, 825–833.
- Xiao, B., & Thomas, K. M. (2004). Competitive adsorption of aqueous metal ions on an oxidized nanoporous activated carbon. *Langmuir*, 20(11), 4566–4578.